Rev. Adv. Mater. Sci. 29 (2011) 83-99

RECENT ADVANCES IN SILICOALUMINOPHOSPHATE NANOCATALYSTS SYNTHESIS TECHNIQUES AND THEIR EFFECTS ON PARTICLE SIZE DISTRIBUTION

Marjan Razavian, Rouein Halladj and Sima Askari

Faculty of Chemical Engineering, Amirkabir University of Technology(Tehran Polytechnic), P.O. Box 15875-4413, Hafez Ave., Tehran, Iran

Received: June 01, 2011

Abstract. This review describes recent developments and achievements in the field of silicoaluminophosphate nanocatalyst production particularly SAPO-11 and SAPO-34. It also explains consequent changes in activity, stability, selectivity, life time and recoverability of some of these new catalysts in different reactions, MTO in particular. SAPO nanoparticles can be obtained by manipulating template, silicon source, heating method, type and time of crystallization, and synthesis conditions like temperature or pressure. Although achieving an ideal dimension, desirable morphology, and mesoporosity resulting in a suitable catalytic performance is still a challenge, all of these investigations point out a unique result which implies considerable enhancements in selectivity, activity and life time on account of size reduction.

1. INTRODUCTION

Because of unique surface properties of catalysts and their ability to influence kinetic of reactions, catalysts are one of the most important issues in the world [1,2]. Although they are used in small amount, they can be contemplated as heart of reactions which makes reactions justifiable economically. Catalysts are responsible for the production of over 60% of all chemicals in the world [3,4]. A huge part of these chemicals are produced in heterogeneous catalytic reactions [5].

Due to the importance of catalysts, especially heterogeneous catalysts, researchers are inclined to produce new catalysts with high quality catalytic performance. This aspiration can be achieved by merging nanotechnology with catalyst industry [6-8]. Therefore the reason of nanocatalysts extension that is associated with their essence of producing extreme surface is clear. Unlike the common practice in catalysis where the catalytic performance scales with the surface to volume ratio of the dispersed catalytic agent, nanocatalysts are distinguished by their unique and non-scalable properties that originate from the highly reduced dimensions of the active catalytic aggregates [7]. Consequently, the essential goal of nanocatalysis is the promotion, enhancement and better control of chemical reactions by changing the size, dimensionality, chemical composition, morphology, charge state of the catalyst or the reaction center, and reaction kinetics [9-13] through nanopatterning of the catalytic reaction centers. Briefly, the importance of particles scale to the catalysts performance has motivated researchers to develop methods for synthesis of selective nanocatalysts with little byproducts and waste output [14-17]. Therefore many alternative techniques for reducing the size of crystals have been represented such as microwave [18] and ultrasound irradiation which has overcome many of the drawbacks found in using conventional

Corresponding author: Rouein Halladj, e-mail: halladj@aut.ac.ir

heating. Two articles about sonochemical synthesis method are available by these authors [19,20].

This review describes all the recent endeavors in producing different SAPO nanocatalysts in the past 10 years. Silicoaluminophosphate molecular sieves are an important member of zeolites family [21-24] which possess considerable potential as acidic catalysts [25] which can play different key roles such as membrane or adsorbent in sorption reactions, template for producing other nanostructured materials and above all, catalyst for petrochemical reactions. It represents condensed descriptions of several routes for synthesis of SAPO-11 and SAPO-34 with small crystals by taking advantage of using different templates, silicon sources, molar compositions, organic base solvents, and crystallization conditions. A brief account is also presented using some of selected examples to illustrate ways that these new nanoforms have advanced heterogeneous catalysis in terms of better control and results of processes. All reports of examining these experimental catalysts suggest that size control of SAPO nanocrystals is a crucial factor in improving the catalytic activity and lifetime of the catalysts.

Text mainly deals with SAPO-34[26-27] synthesis since it is the most investigated one due to its huge application in chemical process especially MTO [28-34], a promising trend in the present economic context [24,35-41]. Production of light olefins such as ethylene and propylene which are key petrochemicals needs a shape selective catalyst [7,42-43] with morphology that provides lots of small entrances and active sites [7]. SAPO-34 is the best catalyst known among silicoaluminophosphates (SAPOs) because of its remarkable pore structure [44], and hydrothermal stability [45] which is dependent on the degree and homogeneity of the silicon incorporated in the chabazite framework [45-50]. Huge amount of investigations about the effect of crystal size showed the best performance for crystals of sizes less than 500 nm [29, 51] in terms of no diffusion limitations during the MTO catalytic reaction.

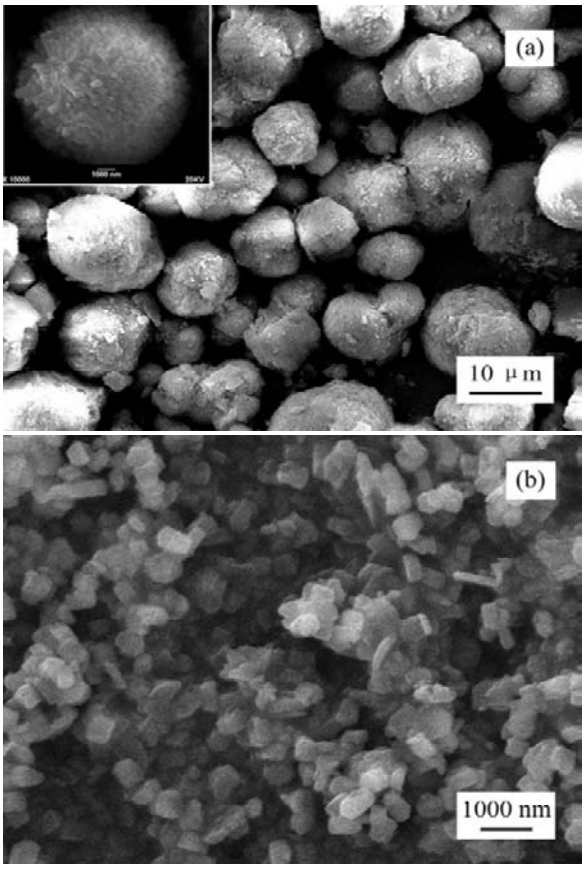

Fig. 1. SEM images of SAPO-11 samples synthesized by the conventional static hydrothermal method (S0, (a)) and the improved static hydrothermal method (S2, (b)) (Adopted from Chinese Journal of Catalysis, Volume 28, Zhang Shengzhen and Chen Sheng-Li and Dong Peng and Ji Zhiyong and Zhao Junying and Xu Keqi, Synthesis and Catalytic Hydroisomerization Performance of SAPO-11 Molecular Sieve with Small Crystals, Pages 857-864, Fig. 1, 2007 copyright with permission from Elsevier).

2. SYNTHESIS TECHNIQUES

2.1. Synthesis of nanoSAPO-11 by taking advantage of aging pretreatment

Generally, SAPO-11 molecular sieves are prepared by the conventional hydrothermal method from gels containing sources of aluminum, phosphorus, and silicon and a structure-directing template such as dipropylamine at crystallization temperatures ranging from 160 to 220 °C for several days. However, crystals of SAPO-11 synthesized from this conventional hydrothermal method normally exhibit large non-uniform pseudospherical aggregates ranging from 3 to 10 μm, sometimes even larger than this size, because of the rapid self-aggregation of the crystal nuclei [52-54]. Ways to synthesize nanometer-sized or submicron-sized SAPO-11 crystals have attracted attentions of worldwide researchers. In 2007, Shengzhen et al. represented one method by making use of aging time pretreatment which helps to obtain more crystalline product with uni-

Table 1. Hydroisomerization performance of *n*-hexadecane over different Pt/SAPO-11 catalysts (Adopted from Chinese Journal of Catalysis, Volume 28, Zhang Shengzhen, Chen Sheng-Li, Dong Peng, Ji Zhiyong, Zhao Junying, Xu Keqi, Synthesis and Catalytic Hydroisomerization Performance of SAPO-11 Molecular Sieve with Small Crystals, Pages 857-864, Table 4, 2007 copyright with permission from Elsevier).

Catalyst	Conversion(%)	Reaction rate[a] (μmol/(g·s))	Reaction rate peracid site[b] (s^{-1})	Product Selectivity (%)			
				i-C_{16}	Mono-C_{16}	Multi-C_{16}	Cracking
Pt/S0	67.8	120.7	0.111	68.1	54.2	13.9	31.9
Pt/S2	89.6	159.6	0.148	82.7	56.6	26.1	17.3

[a] Defined as conversion × molar flow rate/weight of the catalyst.

[b] Defined as reaction rate per Brønsted acid site.

Mono-C16: methylpentadecane; Multi-C16: isohexadecane except for methylpentadecane; Cracking: alkanes less than C16.

Reaction conditions: 340 17.3C, $p(H_2)$ = 8 MPa, $n(H_2)/n$(*n*-hexadecane) = 15, WHSV = 1.5 h^{-1}.

form cubic crystals with the crystal size of 300-600 nm [55] (Fig. 1).

Based on the fact that formation of crystal nuclei takes place at lower temperature, the aging pretreatment of the synthesis gel at room or elevated temperature but below the normal crystallization temperature of SAPO-11 was used to give precursor gel more time to form a large number of nuclei. This pretreatment can make the system homogeneous and generate more seed nuclei, which increase the rate of crystallization. Meanwhile, the nucleation of molecular sieve and the growth of crystals can be affected by the changes in composition and structure of gel during the aging process of initial gels. The topology structures and morphologies of the final products are thereby influenced.

Because aggregation to form large pseudo-spherical particles happens quickly after crystal nuclei formation, controlling the suitable aging time and temperature are two key factors in obtaining SAPO-11 with small crystals. Short aging time leads to impure SAPO-11 products, while a longer aging time can only give big pseudo-spherical particle aggregates [56] and also lower aging temperature is favorable to produce more nuclei, leading to a smaller crystal size of SAPO-11 molecular sieves [57]. In brief, lower temperature and prolonged nucleus formation time is favorable to form a large number of nuclei.

In this part, the aging pretreatment method was used to prepare precursor gel of SAPO-11 with small sub-micron sized crystals without using any other organic additives except the template. The catalytic performance for *n*-hexadecane hydroisomerization of the small SAPO-11 crystals was examined.

This synthesis procedure contains of several steps. The first step was gel preparation by using pseudoboehmite, ortho- phosphoric acid, and silica sol as the sources of aluminum, phosphorus, and silicon, respectively, and a mixture of di-*n*-propylamine (DPA) and/or di-isopropylamine (DIPA) as the structure-directing template under intense stirring. Then the homogeneous mixture, i.e. precursor gel, was transferred into an autoclave and aged at 130–175 °C for 1–6 h without stirring. After the aged gel was cooled down, a specific amount of distilled water was added. This increases the distance between each nucleus and finally decreases the possibility of aggregation which results in smaller average crystal size. In fact, both cool-down and water addition treatments can be mentioned as two another factors besides aging time pretreatment which helped the size reduction procedure by decreasing the temperature and possibility of crystal nucleus aggregation. Silica sol was added next. Then the mixture with molar composition of $1.0P_2O_5$:$1.0Al_2O_3$:$0.4SiO_2$:1.0(DPA+ DIPA) was crystallized at 190 °C for about 24 h. After being cooled, washed, centrifuged, filtrated, and dried, the SAPO-11 molecular sieve with small crystals was obtained.

Considering all these changes, no obvious effect on the acidity of the final product i.e. acid concentration and strength of acid sites, was observed. But these synthesized samples showed larger BET surface area and larger external specific area which make catalysts more reactive.

In addition, Shengzhen used the new synthesized Pt/SAPO-11 (Pt/S2) and the conventional synthesized one (Pt/S0) both in the hydroisomerization of *n*-hexadecane. As it can be seen in Table 1, the hydroisomerization conversion of *n*-hexadecane over the SAPO-11 catalyst with small crystals was 21.8% higher. The total rate and

reaction rate on per acid site were about 1/3 higher than the catalyst supported on the conventional SAPO-11. Besides rate and conversion enhancements, the isomer selectivity especially the selectivity for multi-branched isomers was improved significantly and the yield of hydrocracking as the undesirable side reaction decreased obviously.

The major reason for better catalytic performance of the new synthesized catalyst is attributed to hydroisomerization mechanism of long-chian *n*-alkane. This reaction over SAPO-11 molecular sieve mainly occurs on the external surface of crystals and on the pore mouths. The small crystal SAPO-11 possesses more exposed cell crystals or in the other word pore mouths. The more pore mouths the more available active sites for contacting with reactants, consequently higher catalytic activity. Briefly, small size of crystals shortens the length of products and decreases the diffusion resistance, leading to an improved the isomer selectivity.

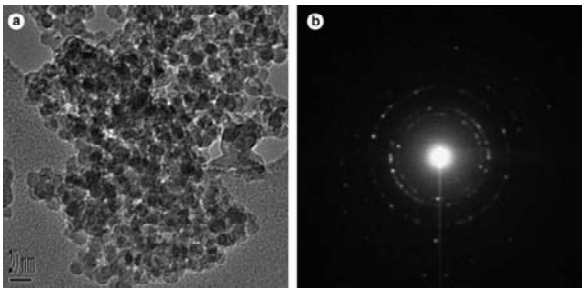

Fig. 2. TEM image of small particle (5-20 nm) aggregates in S-0.29, indicating polycrystalline structures (Adopted from Microporous and Mesoporous Materials, Volume 85, Jianfeng Yao and Huanting Wang and Simon P. Ringer and Kwong-Yu Chan and Lixiong Zhang and Nanping Xu, Growth of SAPO-34 in polymer hydrogels through vapor-phase transport, Pages 267-272, Fig. 4, 2005 copyright with permission from Elsevier).

2.2. Synthesis of nanoSAPO-34 via a pre-shape treatment using a hydrogel polymer

In 2005, Yao group reported a new synthesis method [58] for a fine dispersion of sub-micron or nanosized SAPO-34 crystals with a good degree-of-crystallinity by a novel vapor-phase transport (VPT) process that exploited the three-dimensional network structures of a polymer hydrogel .VPT method generally implements in an autoclave equipped with a porous plate. Crystallization starts via the contact of initial gel with vapor obtained from the liquid mixture which has been poured into the bottom of autoclave. In this case, VPT technique was preferred to hydrothermal method because it generally provides higher zeolite yield, generates less waste and requires less reactor volume. Cross-linked polyacrylamide (C-PAM) hydrogels were employed as mentioned polymer structures to reduce the crystal size of SAPO-34 molecular sieves [59,60]. In fact, this helped SAPO-34 to crystallize within the three-dimensional polymer hydrogel network [61], producing small crystals. A wide size distribution of SAPO-34 crystals, ranging from a few nanometers to 3–5 μm, was obtained when the synthesis precursor gels contained the appropriate amount of C polyacrylamide (C-PAM) hydrogels. These crystals exhibited a BET surface area of 342–325 m^2/g and micropore volume of 0.15–0.12 cm^3/g. Analyses revealed the presence of residual precursor materials, such as phosphorus, supporting the fact that these samples possessed a lower BET surface area and micropore volume as compared with the SAPO-34 prepared by hydrothermal method.

For producing SAPO-34 according to this method, firstly, the typical synthesis gels with a molar composition of $0.75SiO_2$:$1Al_2O_3$:$0.94P_2O_5$:$0.59TEA$:$37.5H_2O$ were prepared by mixing aluminum isopropoxide, phosphoric acid, 30% colloidal silica solution, triethylamine, and deionized water at room temperature for 2–3 h. The uniform precursor gel was then heated to 60 °C under stirring to form dry gels. To study the effect of polymer content on SAPO-34 crystallization, an organic polymer was introduced by adding a mixture of organic monomers (acrylamid: N'-methylenebisacrylamide: ammonium persulfate) to yield synthesis gels having a molar composition of $0.75SiO_2$:$1Al_2O_3$:$0.94P_2O_5$:$0.59TEA$:$37.5H_2O$:xAM (x = 0, 0.29, 0.43, 0.57, 1.15, respectively). The samples obtained from these gels were denoted as S-0, S-0.29, S-0.43, S-0.57, S-1.15, respectively. The organic monomers polymerized at 90 °C so as to solidify the synthesis gels. The solid gel was subsequently transferred into a reactor which was shelved on an autoclave that included the solution of $1TEA$:$10H_2O$ (by mole). Autoclaving was carried out at 170 °C for 48 h to crystallize the precursor into SAPO-34. Finally, the product was calcined at 550 °C for 5 h at the rate of 1 °C /min to remove the polymers and the organic templates.

SEM images of the calcined samples showed the typical SAPO-34 morphology e.g. cubic crystals in the size range of 3-5 μm for S-0 and a distinctly different morphology of small particle aggre-

gates for the other samples. TEM image of the sample S-0.29 (Fig. 2) also indicates that the small particles were ~5–20 nm in size. Therefore, it can be pointed out that with increasing x, the size and external surface area of the crystals decreased and increased respectively. When $x = 0.43$, no micron-sized crystals were found but the degree of crystallinity and surface area and micropore volume decreased. Further increase in C-PAM amount ($x \geq 0.57$) resulted in amorphous products. Therefore, the higher density of C-PAM networks formed by adding more monomers gave rise to a lower degree of crystallinity and smaller crystal size. Consequently, the appropriate amount of C-PAM hydrogel networks (x) to obtain highly crystalline submicron-sized SAPO-34 crystals including nanoscale particles can be suggested in the range of 0.29-0.43.

2.3. Synthesis of nanoSAPO-34 by mixed template method

Precise selection of template is of great significance due to its effect on pore structure, the size of the mesopores, and the pore size distribution [50,62]. Usually SAPO-34 catalysts are fabricated by a single agent like morpholine or tetraethyl ammonium hydroxide (TEAOH) as template. However, using a single SDA in SAPO-34 synthesis, results in rapid coke formation during MTO reaction [26,63-66].The coke would cover acidic sites (place of DME conversion to olefins) and block the pores of SAPO-34 which finally leads to catalyst deactivation. Since 1992, lots of efforts have been made to obtain high performance catalytic materials especially SAPO-34 by using two or more SDAs simultaneously. Sometimes the second template was used just to modify the PH but many of these attempts were to reduce the need for TEAOH by substituting less-expensive amines. All these attempts were successful in decreasing the crystallite size and increasing thermal stability and performance of catalysts, but no nanoscale particle was observed. In 2007, Lee et al. explained that the variety in morphology, crystal size and structure of SAPO catalysts can be achieved by using a mixture of morpholine and TEAOH as the template [67]. Compared with using a single template, a mixed template leads to the particle size reduction and the morphology change to spherical type formed by the aggregation of nano-sized crystals. Besides, the performance parameter of SAPO-34 catalysts, namely catalyst stability was found to be affected by the preparation parameters during synthesis which are closely related with crystal size and the silicon contents during synthesis.

In this case, the silicoaluminophosphate (SAPO) molecular sieve catalysts were synthesized hydrothermally using the mixtures of morpholine and tetraethylammonium hydroxide as a template via a suitable modification of the method reported by Prakash in 1994 [68]. The molar composition for synthesis of the catalysts was kept as $1.0Al_2O_3:1.0P_2O_5:0.6SiO_2:x$morpholine:$(2.0-x)$ TEAOH: $52H_2O$ ($x = 2.0$, 1.8, 1.5, 1.0, 0.5, and 0.0). The synthesis procedure for gel preparation in typical experiment with $x = 1.0$ is described as below.

Pseudoboehmite was added to water and then a mixture of phosphoric acid and water was added to the alumina solution under stirring by a drop-wise addition for 2 h and then the resulting solution was stirred for 2 h at room temperature. Clear silica solution was further added, which was prepared by dissolution of colloidal silica into 35% TEAOH aqueous solution at 100 °C for 12 h by stirring. Finally, morpholine and water was added and the resulting mixture was stirred for 25 h. The resulting gel mass was transferred into autoclave and heated in two steps of 120 and 200 °C and maintained for 12 h at each temperature with vigorous stirring. The solid product was recovered by centrifugation, washed several times with distilled water and dried overnight at 120 °C . As-synthesized product was then calcined in air at 550 °C .

Results showed decrease in crystallinity of SAPO-34 with increase in TEAOH concentration. When TEAOH was only used as a template agent without using morpholine, the major product was SAPO-5 (92%) with presence of minor SAPO-34 (8%) due to high Si content in mentioned experimental conditions. It was also observed that the reduction of Si content during synthesis of gel to half under the same synthesis conditions led to the formation of only pure SAPO-34 phase. Table 2 presents the summary of preparation conditions and phase data.

Also the results showed decrease in surface area from 772 to 284 m^2/g when TEAOH content increased from $x = 0$ to $x = 2.0$ during the synthesis of gel because of the crystallinity lost. Sharp decrease in surface area in the M0 sample (from 623 m^2/g in M10 sample to 284 m^2/g) can be possibly related to the crystal phase change from CHA- to AFI- type. Generally CHA-type molecular sieve has larger BET surface area than those with AFI. In addition, NH_3-TPD results showed decrease in strong acidic sites with increase of TEAOH content while there was no obvious difference in weak acidic sites

Table 2. Preparation conditions for SAPO-34 samples and their confirmed phase (Adopted from Applied Catalysis A: General, Volume 329, Yun-Jo Lee and Seung-Chan Baek and Ki-Won Jun, Methanol conversion on SAPO-34 catalysts prepared by mixed template method, Pages 130-136, Table 1, 2007 copyright with permission from Elsevier).

Sample	Gel composition[a] (*x*)	Temperature (°C)	Time (h)	Product Phase
M20	2.0	200	12	SAPO-34
M15	1.5	200	12	SAPO-34
M10	1.0	200	12	SAPO-34
M5	0.5	200	12	SAPO-34
M0	0	200	12	SAPO-5(92%) + SAPPO-34(8%)

[a]1.0Al2O3:1.0P2O5:0.6SiO2:*x*morpholine:(2-*x*)TEAOH:52H_2O, where *x* is defined as the mole ratio of morpholine to alumina.

Table 3. Product distribution and catalyst lifetime on SAPO catalysts in methanol conversion reaction[a] (Adopted from Applied Catalysis A: General, Volume 329, Yun-Jo Lee and Seung-Chan Baek and Ki-Won Jun, Methanol conversion on SAPO-34 catalysts prepared by mixed template method, Pages 130-136, Table 3, 2007 copyright with permission from Elsevier).

Samples	Catalyst lifetime (min)	MeOH conversion (%)	Product yields (%)			
			C_2^{2-}	C_3^{2-}	C_4^{2-}	Saturated HCs
M20	160	100	42.8	39.1	8.0	10.2
M15	840	100	45.6	36.2	6.2	4.1
M10	520	100	44.6	37.4	6.6	3.0
M5	430	100	42.4	33.9	6.2	3.3
M0	370	100	19.9	40.3	16.0	5.5

[a] Catalyst = 0.49 g of H-SAPO-34, WHSV(MeOH) = 1 h^{-1}, MeOH:He = 1:11 (mol/mol), reaction temperature = 450 °C.

with TEAOH amount. Also it was found that Si content in products increased with an increase in TEAOH amount which is apparently in contrast with earlier result. More investigations showed that some part of Si in M15, M10, and M5 samples remained amorphous in extra-framework and increased in proportion to TEAOH amount.

According to SEM images in Fig. 3a, M20 sample exhibited the rhombohedral shape of typical SAPO-34 with average particle size of 5–20 μm, which is typical when morpholine is used as a template agent [69]. M15 sample, however, showed spherical aggregates of nano-sized cube type SAPO-34 crystals where the aggregates showed average crystal size of 1 μm with homogeneous size distribution. M10 as-synthesized sample (with morpholine and TEAOH in equal amounts) showed irregular shape in morphology with crystal size in sub-micrometer range. The M5 sample showed very interesting morphology where the surface of spherical shaped particle was aggregated with SAPO-34 and M0 sample showed hexagonal type crystal habit which is typical SAPO-5 morphology.

As it can be concluded from Table 3, all these catalysts had complete conversion of methanol and mostly conversion to light olefins in MTO reaction Except for M20 catalyst which showed high yield in saturated hydrocarbons. M15, M10, and M5 samples showed very similar product distributions with high yield in light olefins while M0 catalyst showed different product distribution with relatively high yield in C_4 and C_3 olefins. The lifetime (here 'catalyst lifetime' is defined as time sustaining catalyst activity until total yield of C_2–C_4 olefins exceeds 70%) was in order of M15 > M10 > M5 >M0 > M20 which means that M15 maintained its activity more than the other ones for 840 min. The lifetime was increased by five times compared to that of the cata-

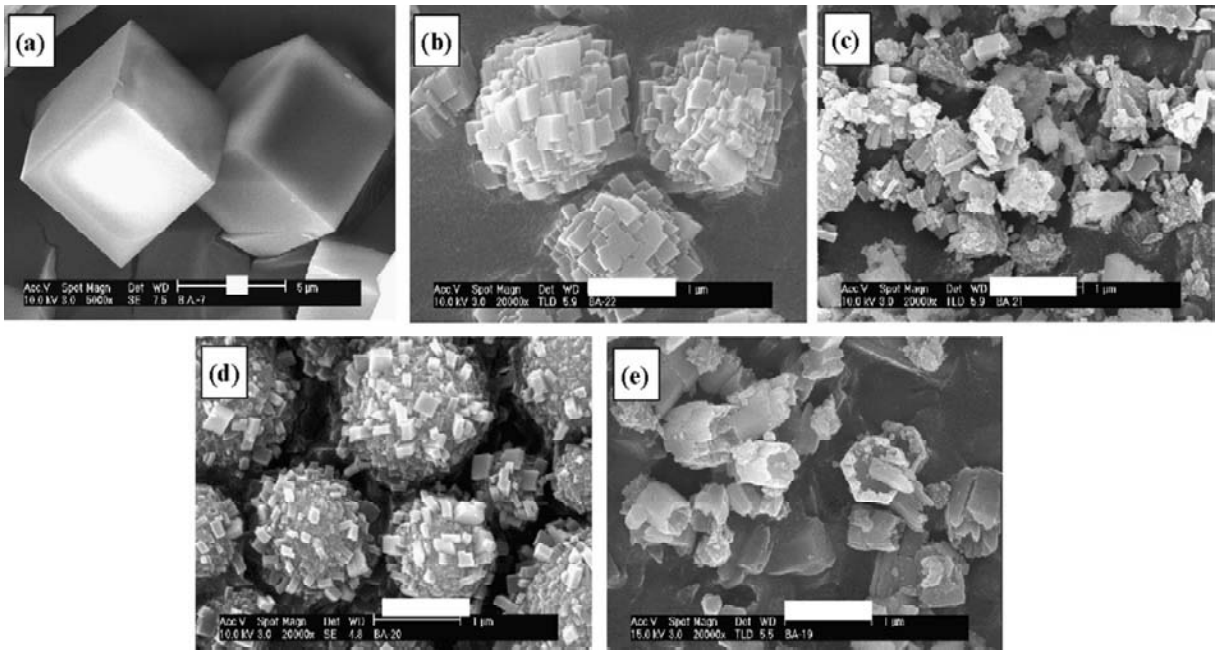

Fig. 3. SEM images of the prepared SAPO samples: (a) M20, (b) M15, (c) M10, (d) M5 and (e) M0. Bars correspond to 1 μm (Adopted from Applied Catalysis A: General, Volume 329, Yun-Jo Lee and Seung-Chan Baek and Ki-Won Jun, Methanol conversion on SAPO-34 catalysts prepared by mixed template method, Pages 130-136, Fig. 2, 2007 copyright with permission from Elsevier).

lyst synthesized with 100% morpholine which is all related to crystal size effect because all samples had similar acidic properties and same crystal structure of CHA topology. In fact, small pore molecular sieves with big crystals possess long intracrystalline diffusion paths that limit the diffusion of reactants and products which may result in coke formation and subsequently deactivation of the catalyst.

2.4. Synthesis of nanoSAPO-34 from colloidal solutions

Another effective factor which is steel under investigation is the type of silicon source. Mertens et al. in 2004 [70] proposed tetaalkyl orthosilicate as a great substitution for silica powder for the first time. Also,Van Heyden team in 2008 [71] reported synthesis of SAPO-34 nanoparticles with diameters less than 500 nm by taking advantage of colloidal precursor solutions in the presence of tetraethylammonium hydroxide as the template.

Clear precursor solutions with molar compositions of $1Al_2O_3$:2–$4P_2O_5$:0.6–$1SiO_2$:2–$4TEA_2O$:75–$147H_2O$ were prepared by mixing Aluminum isopropoxide, colloidal silica, and tetraethylammonium hydroxide solution as SDA at room temperature under stirring for at least 2 h. It is better to keep solution neutral, as the SAPO-34 phase crystallizes most preferentially under slightly acidic or neutral conditions [68]. So, phosphoric acid was added but very slowly during a period of 60-150 min to avoid the formation of dense gel particles. After this level, mixture was treated with stirring for a period of 30 min and was conveyed to the oven. In order to study the crystal growth mechanism of SAPO-34, different samples were synthesized according to the information given in Table 4 in both conventional and microwave ovens and were quenched with cold water after the synthesis time. Then, the suspensions containing nanosized crystals were purified in a series of three steps consisting of high-speed centrifugation, removal of the supernatant, and redispersion in aqueous KOH solution (pH = 8) using an ultrasonic bath. In case of obtaining no material, NaCl solution was used to make a pre-coagulation before centrifugation. Finally, samples were freeze-dried to avoid agglomeration.

All investigated products showed narrow particle size distributions and the resultant suspensions were electrostatically stabilized in basic media. The kinetic study was consistent with a mechanism of crystallization: upon heating of the clear precursor mixtures the dissolved Al-, P-, and Si- sources start to react and form precursor species until a certain degree of super saturation, which is dependent on composition and temperature of heating. Then, nucleation of primary particles takes place within the amorphous species and the particles condense

Table 4. Synthesis conditions and resulting products (Adopted from Chemistry of Materials, Volume 20, Hendrik van Heyden and Svetlana Mintova and Thomas Bein, Nanosized SAPO-34 Synthesized from Colloidal Solutions, Pages 2956-2963, Table 1, 2008 copyright with permission from American Chemical Society).

Sample name	Precursor comp. (Al_2O_3:P_2O_5:SiO_2:TEAO_2O:H_2O)	*T*(°C)	*t*(h)	Structure type code	Particle diameter[a] (nm)	Product Comp Al	P	Si	P+Si
160_2_1	1:2:0.6:2:75	160	0.50	amorphous					
160_2_2	1:2:0.6:2:75	160	1.00	amorphous					
160_2_3	1:2:0.6:2:75	160	1.50	AEI	230	0.51	0.45	0.04	0.49
160_2_4	1:2:0.6:2:75	160	2.00	AEI	240	0.51	0.47	0.02	0.49
160_3_1	1:3:0.6:3:111	160	1.30	amorphous					
160_3_2	1:3:0.6:3:111	160	2.50	amorphous					
160_3_3	1:3:0.6:3:111	160	3.50	amorphous					
160_3_4	1:3:0.6:3:111	160	5.75	CHA(AEI)	320	0.50	0.45	0.05	0.50
160_3_5	1:3:0.6:3:111	160	20.00	CHA	356	0.49	0.45	0.08	0.51
160_4_1	1:4:0.6:4:147	160	2.50	amorphous					
160_4_2	1:4:0.6:4:147	160	3.50	AEI	299	0.50	0.47	0.03	0.50
160_4_3	1:4:0.6:4:147	160	5.00	AEI	329	0.51	0.46	0.03	0.49
160_4_4	1:4:0.6:4:147	160	13.50	AEI	340	0.50	0.46	0.04	0.50
160_4_5	1:4:0.6:4:147	160	15.00	CHA	417	0.50	0.42	0.08	0.50
180_2/1_1	1:2:1:2:77	180	0.50	amorphous					
180_2/1_2	1:2:1:2:77	180	1.00	amorphous					
180_2/1_3	1:2:1:2:77	180	1.50	CHA (low yield)	181				
180_2/1_4	1:2:1:2:77	180	2.00	CHA	285	0.51	0.42	0.07	0.49
180_2/1_5	1:2:1:2:77	180	2.50	CHA	272	0.52	0.42	0.06	0.48
180_2_1	1:2:0.6:2:75	180	0.50	amorphous					
180_2_2	1:2:0.6:2:75	180	1.00	amorphous					
180_2_3	1:2:0.6:2:75	180	2.00	CHA	286	0.51	0.42	0.07	0.49
180_2_4	1:2:0.6:2:75	180	4.25	CHA	316	0.52	0.42	0.06	0.48
180_3_1	1:3:0.6:3:111	180	2.00	amorphous					
180_3_2	1:3:0.6:3:111	180	3.00	CHA	264	0.50	0.47	0.03	0.50
180_3_3	1:3:0.6:3:111	180	4.00	CHA	265	0.50	0.46	0.04	0.50
180_3_4	1:3:0.6:3:111	180	6.00	CHA	276	0.49	0.45	0.05	0.51
180_3_5	1:3:0.6:3:111	180	18.50	CHA	507	0.49	0.44	0.08	0.51
180_4_1	1:4:0.6:4:147	180	2.00	amorphous					
180_4_2	1:4:0.6:4:147	180	3.00	amorphous					
180_4_3	1:4:0.6:4:147	180	4.50	CHA	308	0.51	0.46	0.03	0.49
180_4_4	1:4:0.6:4:147	180	5.50	CHA	350	0.51	0.46	0.03	0.49
180_4_5	1:4:0.6:4:147	180	7.00	CHA	368	0.51	0.45	0.04	0.49
180_2_MW	1:2:0.6:2:75	180	7.25	CHA	206	0.50	0.41	0.09	0.50

[a] Particle diameters are given as *Z*-average values of the corresponding Cumulants algorithm.

and form crystalline aggregates. Simultaneously, these particles grow by further addition of nutrients from the synthesis solution until they reach their final size. Additionally, at a relatively later stage of heating, aggregation and condensation of secondary particles or Ostwald ripening take place.

In order to obtain small crystals, it is important to balance the size of primary particles and the proceeding growth rate by careful adjustment of synthesis conditions. According to all results, particle size affecting parameters can be summarized in 3 items: 1- Synthesis time after hydrothermal treat-

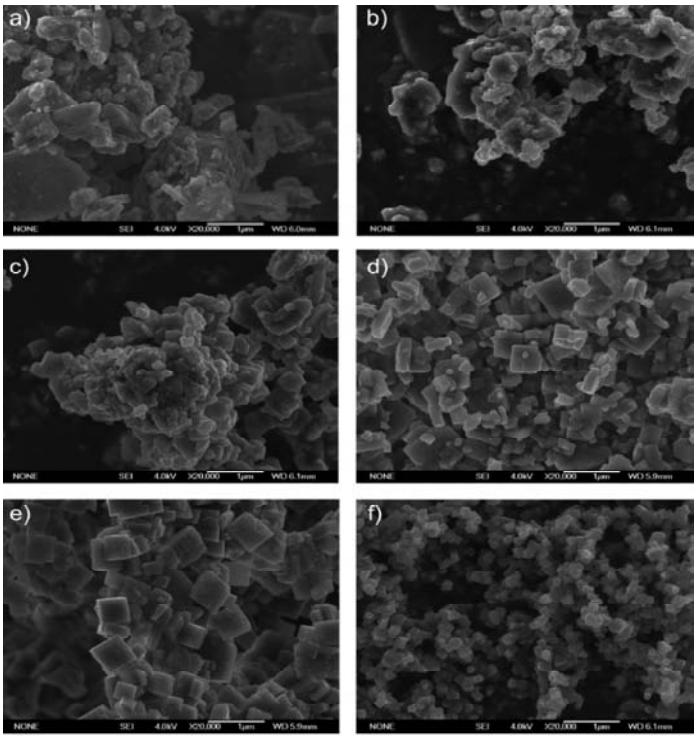

Fig. 4. SEM images of samples 180_4_1–180_4_5 (a–e) and 180_2_MW (f) (Adopted from Chemistry of Materials, Volume 20, Hendrik van Heyden and Svetlana Mintova and Thomas Bein, Nanosized SAPO-34 Synthesized from Colloidal Solutions, Pages 2956-2963, Fig. 4, 2008 copyright with permission from American Chemical Society).

ment: Prolonging the synthesis time resulted in bigger crystals even aggregates up to 1 μm. 2- Concentration of precursor solution: Fast and homogeneous nucleation happened in more concentrated systems because of the high degree of supersaturation during the induction heating period [72]. 3- The elapsed time between nucleation and quenching.

As it can be concluded from Table 4, these three factors have effects not only on the morphology but also on the crystal size. SEM images of the 180-4 series samples that are shown in Fig. 4 confirm this fact. Figs. 4a and Fig. 4b show agglomerated particles with undefined morphology. The size of individual flocculated particles at higher magnification estimated about 100 nm. Figs. 4c-4e demonstrates crystals with typical SAPO-34 structure for the samples 3–5 without any impurity in contrast with samples which were crystallized at 160 °C. Therefore with increasing crystallization time, cubic like crystals with bigger particle size were obtained. Moreover, temperature is reckoned to play an important role in obtaining pure SAPO-34 products. Nearly all samples which were synthesized at 160 °C contained both AEI (SAPO-18) and CHA-type materials. However, recrystallization from AEI to CHA was observed in these systems with increasing the time of heating.

2.5. Synthesis of SAPO-34 nanocrystals by dry gel conversion method

Dry gel conversion, a new technique for the synthesis of zeolites [73-76], AlPO, and SAPO [77-79], has been extensively studied by several groups. Hirota et al. in 2010 [80] accomplished to synthesize nanocrystals of SAPO-34 by a dry gel conversion using tetraethylammonium hydroxide (TEAOH) as a structure-directing agent (SDA). The average crystal size of resultant SAPO-34 was 75 nm, which is significantly reduced in comparison with previous samples which were prepared by this team by hydrothermal method using the same SDA(800nm) [81]. This method suggests a much higher nucleation density in the early stages of synthesis and slow crystal growth after nucleation than that under hydrothermal conditions. One more thing is that the full crystallinity was observed after 6 hours while in hydrothermal treatment at least 24 hours was required to obtain fully crystalline SAPO-34 crystals. These results indicate that dry gel conversion is a

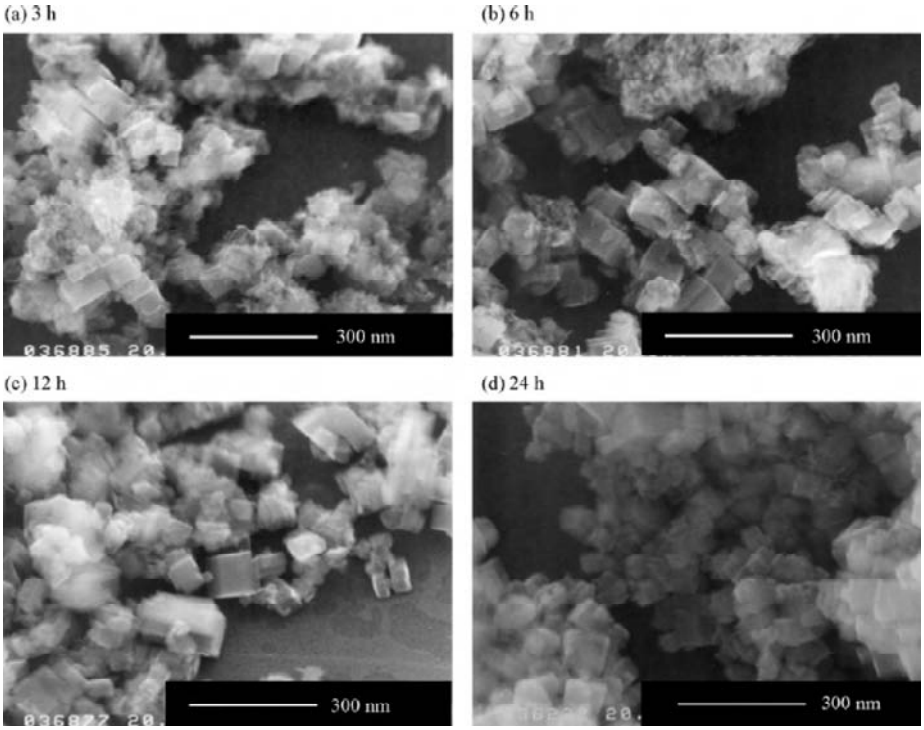

Fig. 5. FE-SEM images of DGC-SAPO-34 Adopted from Materials Chemistry and Physics, Volume 123, Yuichiro Hirota and Kenji Murata and Shunsuke Tanaka and Norikazu Nishiyama and Yasuyuki Egashira and Korekazu Ueyama, Dry gel conversion synthesis of SAPO-34 nanocrystals, Pages 507-509, Fig. 2, 2010 copyright with permission from Elsevier).

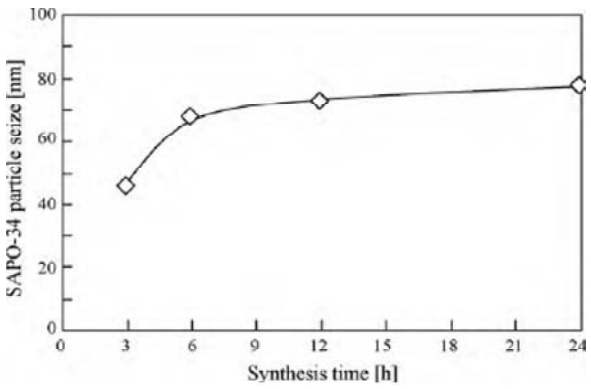

Fig. 6. Crystal size of DGC-SAPO-34 as a function of the synthesis time (Adopted from Materials Chemistry and Physics, Volume 123, Yuichiro Hirota and Kenji Murata and Shunsuke Tanaka and Norikazu Nishiyama and Yasuyuki Egashira and Korekazu Ueyama, Dry gel conversion synthesis of SAPO-34 nanocrystals, Pages 507-509, Fig. 4, 2010 copyright with permission from Elsevier).

very useful technique for the synthesis of SAPO-34 nanocrystals in a high yield.

Production of SAPO-34 based on this method started with mixing of Boehmite (AlOOH) and phosphoric acid as sources of aluminum and phosphorous. Colloidal silica containing 30 wt.% of SiO_2 and 0.4 wt.% of Na_2O was used as the source of silicon. A 20 wt.% aqueous solution of TEAOH was used finally as the SDA. The initial gel with following molar ratio of $1.0Al_2O_3$:$1.0P_2O_5$:0.6 SiO_2:1.8TEAOH:$77H_2O$ was stirred for 24 h at 30 °C , and then dried at 90 °C to give a dry gel. This drying before crystallization induces further nucleation at the stage of dry gel conversion. The dry gel was placed in a vessel and a small amount of water that served as a source of steam was separately added to the same vessel. Crystallization was conducted at 180 °C for 1.5–24 h. The products were rinsed with deionized water and finally calcined at 600 °C for 6 h.

It is obvious of the SEM images in Fig. 5 that all samples showed cubic crystals with no amorphous phase, suggesting a high degree of crystallinity for the SAPO-34. Fig. 6 shows a plot of the sizes of the SAPO-34 crystals, based on SEM measurements, as a function of the synthesis time. As it is shown, after 3 h, 45 nm SAPO-34 crystals containing an amorphous phase were observed. The crystal size increased to 70 nm after 6 h and did not increase significantly after further synthesis.

MTO and DTO (Dimethylether-to-olefins) reactions were conducted over SAPO-34 nanocatalysts

which have been prepared through dry gel technique (DGC-SAPO-34) and conventional procedure, i.e. hydrothermal synthesis method (HTS-SAPO-34) [82] .The DGC-SAPO nanocatalyst was found to be more acidic in comparison with HTS-SAPO and showed a higher dimethylether conversion and higher selectivity towards light olefins for the DTO and MTO reactions, respectively. Also, it exhibited longer catalyst lifetime compared to HTS-SAPO catalyst. That can be related to various reasons including different effectiveness factor (=observed reaction rate/reaction rate without diffusion resistance) and competitive diffusion of olefins with MeOH or DME to reenter the pores of catalyst. The rate of coke deposition on DGC-SAPO was slower compared to HTS-SAPO catalyst for both the MTO and DTO reactions. However, the amount of coke deposition was larger on DGC-SAPO-34.

2.6. Synthesis of nanoSAPO-34 by taking advantage of microwave heating

Lots of researches in last years have been focused on investigating the importance of different synthesis factors such as the silica source, water content, crystallization time and aging time on the crystal size and shape of the silicoaluminophosphate molecular sieve SAPO-34. Some of literatures related to mentioned items have been explained in previous sections. Recently, Lin et al. [83] has fabricated SAPO-34 nanoparticles with controlled shape and size through choosing various source of silica, the H_2O/Al_2O_3 molar ratio, the crystallization and aging time in the reaction system of Al_2O_3–P_2O_5–SiO_2–TEAOH–H_2O under microwave radiation.

In this study, the SAPO-34 crystals with different morphologies i.e., nano sheet-like crystals, uniform nanoparticles and microspheres were synthesized by microwave heating from the reaction mixture of $1.0Al(OPr^i)_3$:$2.0H_3PO_4$:2.0TEAOH: $0.3SiO_2$:(30–120)H_2O. Aluminum isopropoxide $Al(OPr^i)_3$ was firstly mixed with TEAOH solution and deionized water at room temperature until dissolved completely. Silica source [tetraethylorthosilicate (TEOS), colloidal silica or SiO_2 powder] was then added and stirred for 2 h. Finally, phosphoric acid was dispersed slowly into the above solution. The reaction mixture was further stirred for 1 h and then transferred into an autoclave. The crystallization was conducted in a microwave oven with pre-programmed heating profiles at 180 °C for 1h. The product was separated by high speed centrifugation, washed thoroughly with deionized water and ethanol, and then dried overnight at 50 °C. The as-synthesized crystals were calcined at 550 °C in air for 6 h to remove the template molecules.

Results of different analyses on products revealed that the morphology and the sizes of crystals are dependent on H_2O/Al_2O3 molar ratio, aging time, crystallization time, and silica source in particular. For better understanding of the effect of synthesis parameters mentioned above, four parts explaining these factors in details are prepared below.

The influence of silica source on morphology is attributed to two terms of different solubility and reactivity rate of silica source in alkaline medium. Using both of the colloidal silica and solid SiO_2 powder resulted in same product, e.g. SAPO-34 nanocrystals with sheet-like morphology but a little more aggregated in the sample which was prepared using SiO_2 powder as the silica source. Also, substitution of tetraethyl orthosilicate for colloidal silica or SiO_2 powder changed the morphology of particles to a shape of irregular spheres significantly and produced uniform nanoparticles with sizes of about 100 nm.

For a comparison, the reaction of Al_2O_3–P_2O_5–TEOS–TEAOH–H_2O was also carried out by conventional heating at 180 °C. As it is shown in Fig. 7, the product was pure SAPO-34 but with less uniform and more aggregated crystals compared to the particles formed by microwave heating.

To study the effect of water content on the morphology of SAPO-34 crystals, the H_2O/Al_2O_3 molar ratio was adjusted from 30 to 120 in the reaction mixture. Results suggested no relation between morphology and sizes of crystals with H_2O/Al_2O_3 molar ratio when colloidal silica or SiO_2 powder was used as the silica source. In contrast, using TEOS led to a dramatic change of morphology from nanoparticles to microspheres with increasing of the H_2O/Al_2O_3 molar ratio which reminds of the importance of silica source as a crucial factor again. The change of the crystal morphology from nanoparticles to microspheres might be attributed to the decrease of the supersaturation of the precursor solution with increase of water content.

To further investigate the formation of the SAPO-34 particles, another two important factors including crystallization and aging time were studied. SEM images of the SAPO-34 crystals which were synthesized with different aging periods (2, 12, 36, 48, and 60 h) before the addition of the phosphoric acid showed that aging time is an effective way to reduce the particle size to 60-80 nm. In fact, the effect of aging time on size reduction of particles is related to its influence on the distribution of silica

precursor species. Additionally, SEM images of the samples which were manufactured at different crystallization periods indicated a gradual increase in crystal size of microspheres with prolonging crystallization time, the usual manner which has been observed in all other works. The critical time for the formation of the nanosized particles can be estimated below 40 min. Further increasing the crystallization time to 2 h, the crystals grew into micro scale spheres. Meanwhile, the obtained microsphere surfaces became rougher with the increase of crystals size. However, prolonging the crystallization time to 2.5 h resulted in the decrease of microspheres in size.

3. GENERAL OVERVIEW AND COMPARISON

All different techniques which have been presented in obtaining SAPO nanocrystals up to now were explained in detail. Here, we will give a broad outline of these methods covering major points and their results to be able to compare methods at the end.

From practical considerations it can be concluded that accurate selection of structure-directing agent has critical influence on the morphology, size of the mesopores, and the pore size distribution. A double or triple mixture of different templates also can yield a huge decrease in particle size which strongly influences the catalytic properties especially catalyst stability and lifetime. Applying this technique in manufacturing SAPO-34 by using tetraethyl ammonium hydroxide and morpholine mixture as the SDA produced satisfactory results in obtaining small crystals with sizes of several hundred nanometers, in contrast with cubic crystals with few microns in size, which have been produced through using a single template. It demonstrates the importance of not only the type but also the size of template molecules in producing desirable uniform tailored structure. In other word, by using larger template molecules the mesopores size increases and the pore size distribution becomes broader. In addition, template concentration has strong influence on products final morphology and degree of crystallinity. Also, employing a crystal growth inhibitor like polyethylene glycol or methylene blue besides using mixed template can intensify size reduction procedure. It creates conditions that favor nucleation over crystal growth and produces a large number of small nuclei. Applying this method in SAPO-34 synthesis by Venna et.al [84] resulted in high surface area SAPO-34 catalyst with small crystal size in the ~600-900 nm range and narrow size distribution.

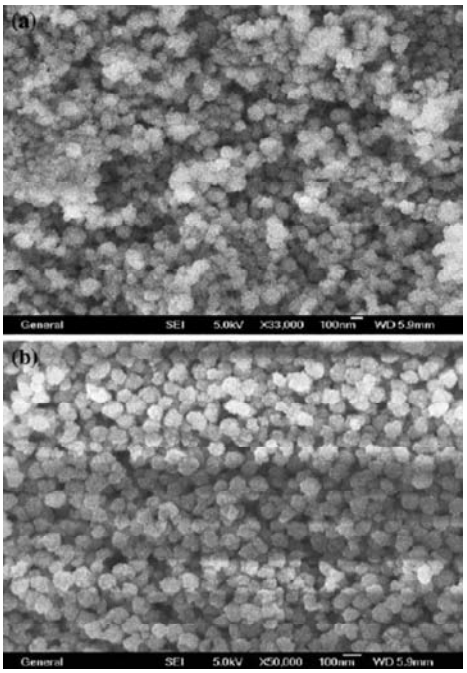

Fig. 7. SEM images of SAPO-34 crystals crystallized by different methods: (a) conventional heating (b) microwave heating (Adopted from Topics in Catalysis, Fabrication of SAPO-34 Crystals with Different Morphologies by Microwave Heating, Volume 53, 2010, Pages 1304-1310, Song Lin, Jiyang Li, Raj Pal Sharma, Jihong Yu, Ruren Xu, Fig. 3 with kind permission from Springer Science+Business Media).

Due to the leading role of SAPO-34 in petrochemical industry, i.e. producing olefins from methanol, most of the investigations have been conducted on manufacturing mild acidic catalyst with small crystals. Controlling the incorporation of Si atoms in the chabazaite framework during crystallization process can boost porosity, surface area, pore volume and consequently catalytic performance including reaction rate and selectivity. SAPO-34 nanoparticles have been synthesized by a variety of different approaches which have resulted in huge size reduction and considerable improvements in catalysts performance. The simplest ways to obtain nanoparticles are related to silicon source manipulation by substituting of tetraalkyl orthosilicate and colloidal silica for powder silica [70] or dissolving the silicon in an organic base solution [85] before mixing with other reagents which led to enormous particle size reduction by forming more nuclei. Van Heyden et al. [71] showed that using colloidal solution creates a high degree of supersaturation at the end of the induction heating period, which brings about fast and homogeneous nucleation of a high number of nuclei with ideal monomodal size distri-

Table 5. Comparison of properties of SAPO samples, obtained from different methods.

Synthesis method	Product phase	Structure	Morphology	Size (nm)	BET surface(m^2/gr)	Pore volume(m^3/gr)
Synthesis of nanoSAPO-11 by taking advantage of aging pretreatment	SAPO-11	AEL	Cubic crystals	400-500	242.2	0.196
Synthesis of nanoSAPO-34 via a pre-shape treatment using a hydrogel polymer	SAPO-34 (S-029)	CHA		5-5000	342	0.25
Synthesis of nanoSAPO-34 by mixed template method	SAPO-34 (M10)	CHA		<1000	665	
Synthesis of nanoSAPO-34 from Colloidal Solutions	SAPO-18	AEI	Sheet-like hexagonal crystals	230-340		
	SAPO-34	CHA	Cubic crystals	181-507		
Synthesis of SAPO-34 nanocrystals by dry gel conversion method	SAPO-34	CHA	Cubic crystals	~75		
Synthesis of nanoSAPO-34 by taking advantage of Microwave Heating	SAPO-34	CHA	Sheet-like crystalsuniform irregular spheresspheres[a]	60-1500		

[a] Any of these three type of morphologies can be obtained according to the type of the silicon source, crystallization and aging time, and H_2O/Al_2O_3 ratio that is used in the synthesis procedure.

bution. However, size reduction in this method happened because of not only the colloidal form of solution but also microwave hydrothermal treatment.

Type of heating method is one of the most crucial aspects in fabricating small crystals which is under research currently and some promising results are emerging. Vapor phase transport and particularly microwave and ultrasonic irradiation seem to be appropriate alternatives for hydrothermal method. They provide high rate and short time of heating which results in uniform homogenous pure products. This high rate creates a fully crystalline product and inhibits any second phase growth as impurity. Meanwhile, lower temperature and shorter time will be needed for calcination in next step in comparison with hydrothermal technique. Till now, just VPT [86-87] and microwave [88,90] method have been examined on SAPO-34 and SAPO-5 and SAPO-11synthesis which yielded great results. As it was mentioned, one of the best results was observed in part 2.4 for obtaining SAPO-34 nanocrystals by using microwave oven along with colloidal form of silicon source. Results of analyses confirmed the fully crystalline cubic structure of product with 100 nm crystals which is significantly decreased in comparison with samples crystallized via conventional ovens. These findings suggest more attempts to investigate the mechanism and whole effects of these methods especially microwave and ultrasonic irradiation which seem to make all the difference. Also dry gel conversion method can be named as efficacious as microwave technique in fabricating SAPO-34 molecular sieve. It includes one more step in comparison with other methods which

is the conversion of precursor solution to a dry gel before crystallization. This method is a great route for the synthesis of zeolites especially those that are not possible to be produced via the hydrothermal crystallization method with less required synthesis time and expensive templates. It is worth mentioning that the amount of water present in the autoclave during the crystallization process is a critical factor in obtaining highly crystalline products.

SAPO-11 cubic nanoparticles were manufactured by exploiting an aging time pretreatment before crystallization step. It gave time to generate more nuclei which increased the rate of crystallization. It changed final topology as well, as leading to a suitable reactive catalyst with higher surface area than sample prepared conventionally. This method is an effective economical way which cause decrease in particle size impressively. But aging temperature and time should be chosen precisely as two key factors to attain a noble design of catalyst. Also, SAPO-11 crystals with sizes between 500-1000 nm were synthesized through a combined method using an alcohol like isopropyl alcohol as the dispersing agent, the mixture of n-dipropylamine and iso-dipropylamine as SDA, and aging pretreatment [91].

Besides, there are several minor but important hints which can help the process of size reduction within the other major methods. Duration of phosphoric acid addition in synthesis procedure, exact estimation of water content in the synthesis mixture, exploiting an autoclave with shaking ability, adding water after cool-down treatment and using any kind of organosilane as an organic ligand in surface functionalizing can be pointed out as these hints. Phosphoric acid is needed for neutralizing precursor media to prepare appropriate PH, but it should be added drop-wise over a period of ~2 hr to avoid the formation of dense gel particles. Water proportion to other reactants should be calculated carefully because of its effect on the supersaturation of the precursor gel. Low degree of supersaturation leads to less nucleation sites and formation of big particles. Using agitator or an autoclave with shaking ability prevents agglomeration and produces more small crystals. Also, water can be added to gel as a diluting agent after some hours being placed in autoclave. This increases the distance between each nucleus and finally decreases the possibility of aggregation. And as the final point, surface functionalizing method should be mentioned as an effective way to prevent or reduce agglomeration and pores disorder during calcination [92]. It includes grafting organic functional ligands such as an organosilane on the surface of as-synthesized template-containing colloidal molecular sieve nanoparticles and removing the structure-directing template by calcination.

A summary of some important data related to these different SAPO materials which have been prepared through mentioned techniques is provided in Table 5.Using of Aging time pretreatment in 2.1 and 2.6 sections were successful in obtaining small pure SAPO-11 and SAPO-34 crystals but it should be combined with another method to produce high surface area and acidic catalysts. Vapor phase transport technique besides using a hydrogel polymer is an appropriate technique for producing small crystals by means of preventing crystal aggregation and preshaping nanostructures. But this technique needs some improvements to give a narrow size distribution and prohibit crystallinity lost which results in lower BET surface area and pore volume in comparison with hydrothermal method. Use of a mixture of several amines as the template can bring a huge size reduction which has a critical influence over the stability of catalyst. This technique is capable of producing high surface area catalyst (up to 772 m^2/gr) with long life time which is one of the positive aspects of size reduction. Small crystals possess short intracrystalline diffusion paths that are not long enough for the conversion of reaction intermediates to coke which is the main reason of catalyst deactivation. It also decreases the incorporation of an expensive template like TEAOH by introducing another one or two cheaper SDAs into the synthesis procedure.

From all these versatile methods which have been represented in this paper, best results has been obtained through dry gel conversion and microwave heating techniques for the synthesis of pure SAPO-34 nanocrystals. They both enhance the nucleation and crystal growth and obtain small crystals with average size of less than 100 nm which is tremendously reduced in comparison with samples which have been manufactured by hydrothermal technique. Also SAPO-34 sample prepared by dry gel conversion showed longer catalyst life time and more acidic properties at most twice as much as sample prepared by hydrothermal method.

4. CONCLUSIONS

The forgoing review offered different synthesis routes in the field of SAPO nanocatalyst production especially SAPO-11 and SAPO-34 which have been under spotlight in the last decade. Also, it provided small abstracts of consequent changes in activity,

stability, lifetime, recoverability and selectivity in particular in some of these methods. All these techniques were based on this fact that for achieving an ideal high performance catalyst, size of particles should be reduced. However, this parameter is not the only factor which must be taken into account to reach high catalytic performance. Improvements in cavity shape and dimensions and diffusion paths or in short term well-defined porous structures are needed as well to remove the limitations. Combination of these two factors has shown significant influence over catalytic properties of SAPO molecular sieves. For instance, in SAPO-34 it resulted in an increase in the ratio of acid sites of the external surface to acid sites in the porous structure which plays an important role in the reduction of the conversion of olefins to paraffins in MTO reaction.

There has been an enormous attempt to accomplish the prospect mentioned above but just some of them have met with some success in recent years. But then again, a number of these methods were successful in obtaining nanoparticles in few last years through manipulating template, silicon source, heating or crystallization method and synthesis conditions.

Authors are aware of the fact that this field of research is still in progress and new concepts are under development but they hope that this collection of new techniques will provide an insight into these new practical fundamentals and be the premise for noble concepts in producing advanced catalysts based on nanopatterns design in future which can entirely omit the limitations.

REFERENCES

[1] M. Baerns, *Basic Principles in Applied Catalysis* (Springer, Berlin, 2004).

[2] V.S. Arunachalam and E.L. Fleischer, *Harnessing Materials for Energy* (MRS Bulletin 33, 2008).

[3] J. Hagen, *Industrial Catalysis: A Practical Approach, 2nd edn.* (Wiley-VCH, Weinheim, 2006).

[4] J.M. White and J. Bercaw, *Opportunities for Catalysis In The 21st Century (*Basic Energy Science Advisory Committee Subpanel Workshop Report, 2002).

[5] J.F.L.E. Page, *Applied Heterogeneous Catalysis: Design, Manufacture, Use of solid catalysts* (Editions Technip, Paris, 1978).

[6] H.H. Kung and M.C. Kung MC, In: *Nanotechnology in Catalysis*, ed. by B. Zhou, S. Han, R. Raja and G.A. Somorjai (Springer, New York, 2007).

[7] C.R. Henry, In: *Nanocatalysis*, ed. by U. Heiz and U. Landman (Springer, Berlin, 2007).

[8] J. Cejka, H. Van Bekkum, A. Corma and F. Schueth, *Introduction To Zeolite Molecular Sieves* (Elsevier Science, 2007).

[9] V.N. Parmon // *Dokl. Phys. Chem.* **413** (2007) 42.

[10] D.Y. Murzin // *Chem. Eng. Sci.* **64** (2009)1046.

[11] J. Sun, *Thermodynamics And Kinetics at the Nanoscale : Thermal Behavior of Aluminum Nanoparticles and Development of Nanoporous Low-K Dielectrics* (Dissertation, Tech. University, Texas, 2004).

[12] Pour A. Nakhaei, M.R. Housaindokht, S.F. Tayyari and J. Zarkesh // *J. Nat. Gas. Chem.* **19** (2010) 441.

[13] V. Seebauer, J. Petek and G. Staudinger // *Fuel* **76** (1997) 1277.

[14] A. Sayari and M. Jaroniec, *Stud Surf Sci Catal 141:Nanoporous MaterialsÉÉÉ* (Elsevier Science B.V., Amsterdam, 2002).

[15] A. Sayari and M. Jaroniec, *Nanoporous Materials V* (World Scientific, Vancouver, 2008), p. 113.

[16] W.R. Moser, *Advanced catalysts and nanostructured materials: Modern synthetic methods* (Academic Press, San Diego, 1996).

[17] N.R. Shiju and V.V. Guliants // *Appl Catal A* **356** (2009) 1.

[18] C.F. Cheng, H.H. Cheng, L.L. Wu and B.W. Cheng, In: *Stud Surf Sci Catal 156: Nanoporous Materials IV*, ed. by A. Sayari and M. Jaroniec (Elsevier Science B.V., Ontario, 2005).

[19] S. Askari, R. Halladj and B. Nasernejad // *Mater. Sci. Poland* **27** (2009) 397.

[20] J. Talebi, R. Halladj and S. Askari // *J. Mater. Sci.* **45** (2010) 3318.

[21] B.M. Locke, C.A. Messina, R.L. Patton, R.T. Gajek, T.R. Cannan and E.M. Flanigen, *US Patent 4440871,* (1984).

[22] E. Furimsky, *Catalysts for upgrading heavy petroleum feeds* (Elsevier Science B.V., Amsterdam, 2007).

[23] J.A. Martenes, I. Balaktishnan, P.J. Grobet and P.A. Jacobs PA, *Zeolite chemistry and catalysis* (Elsevier Science B.V., Amsterdam, 1991).

[24] Z. Liu and J. Liang // Curr. Opin. Solid. ST. M **4** (1999) 80.
[25] R. Shah, J.D. Gale and M.C. Payne // *Phase Trans*. **61** (1997) 67.
[26] J. Liang, H.Y. Li, S.Q. Zhao, W.G. Guo, R.H. Wang and M.Z. Li // *Appl. Catal.* **64** (1990) 31.
[27] S. Wilson and P. Barger // *Micropor. Mesopor. Mater.* **29** (1999) 117.
[28] A.J. Marchi and G.F. Froment // Appl. Catal. **71** (1991) 139.
[29] D. Chen, H.P. Rebo, K. Moljord and A. Holmen // *Ind. Eng. Chem. Res.* **38** (1999) 4241.
[30] M.J. Van Niekerk, J.C.Q. Fletcher and C.T. O'Conner // *Appl. Catal.* **138** (1996) 135.
[31] A.G. Gayubo, A.T. Aguayo, A. E. Sanchez del Campo, AE, Tarrýo and J. Bilbao // *Ind. Eng. Chem. Res.* **39** (2000) 292.
[32] S. Soundararajan, A.K. Dalai and F. Berruti // *Fuel* **80** (2001) 1187.
[33] S.M. Alwahabi and G.F. Froment // *Ind. Eng. Chem. Res.* **43** (2004) 5098.
[34] H. Zhou, Y. Wang, F. Wei, D. Wang and Z. Wang // *Appl. Catal. A* **348** (2008) 135.
[35] C.D. Chang // *Catal. Rev. Sci. Eng.* **25** (1983) 1.
[36] C.D. Chang // *Catal. Rev. Sci. Eng.* **25** (1983) 323.
[37] B.V. Vora, T. Marker, E.C. Amold, H. Nilsen, S. Kvisle and T. Fuglerud, In: *Stud Surf Sci Catal 107: Natural Gas Conversion IV,* ed. by M. Pontes, R.L. Espinoza, C.P. Nicolaides, J.H. Scholtz and M.S. Scurrell (Elsevier Science B.V., 1997).
[38] M. Stöcker // *Micropor. Mesopor. Mater.* **29** (1999) 3.
[39] S.M. Alwahabi, *Conversion of Methanol to Light Olefins on SAPO-34: Kinetic Modeling and Reactor Design* (Dissertation, Texas A&M University, 2003).
[40] L. Jean, *Effect of Process Parameters on Methanol to Olefins Reactions over SAPO Catalysts (*Thesis, Auburn University, Alabama, 2005).
[41] B. Vora, J.Q. Chen, A. Bozzano, B. Glover and P. Barger // Catal. Today **141** (2009) 77.
[42] F.G. Dwyer, In: *Structure-Activity and Selectivity Relationship in Heterogeneous Catalysis,* ed. by R.K. Grasselli and A.W. Sleight (Elsevier Science B.V., Amsterdam, 1991). 179.
[43] I.M. Dahl, H. Mostad,D. Akporiayeand R. Wendelbo // Micropor. Mesopor. Mater. **29** (1999) 185.
[44] J. Park, J.Y. Lee, K.S. Kim, S.B. Hong and G. Seo // *Appl. Catal. A* **339** (2008) 36.
[45] Y. Watanabe, A. Koiwai, H. Takeuchi and S. Hyodo // *J. Catal.* **143** (1993) 430.
[46] M. Popova, C. Minchev and V. Kanazirev // *Appl. Catal. A* **169** (1998) 227.
[47] S. Ashtekar, S.V.V. Chilukuri and D.K. Chakrabarty // J. Phys. Chem. **98** (1994) 4878.
[48] G. Sastre, D.W. Lewis and C.R.A Catlow // *J. Phys. Chem.* **101** (1997) 5249.
[49] G. Sastre, D.W. Lewis and C.R.A Catlow // *J. Mol. Catal.* **119** (1997) 349.
[50] N. Danilina and J.A. Van Bokhoven, In: *Zeolites and Related Materials: Trends, Targets and Challenges*, ed. by A. Gedeon, P. Massiani and F. Babonneau, (Elsevier B.V., Paris, 2008), 213.
[51] D. Chen, K. Moljord, T. Fuglerud and A. Holmen // *Micropor. Mesopor. Mater.* **29** (1999) 191.
[52] P. Meriaudeau, V.A. Tuan, V.T. Nghiem, S.Y. Lai, L.N. Hung and C. Naccache // *J. Catal.* **169** (1997) 55.
[53] J.M. Campelo, F. Lafont and J.M. Marinas // *Zeolites* **15** (1995) 97.
[54] M. Alfonzo, J. Goldwasser, C.M. López, F.J. Machado, M. Matjushin and B. Méndez // *J. Mol. Catal. A* **98** (1995) 35.
[55] Z. Shengzhen, C. Sheng-Li, D. Peng, J. Zhiyong, Z. Junying and X. Keqi // *Chin. J. Catal.* **28** (2007) 857.
[56] M. Liu and S.H. Xiang // *Acta Petrol. Sin.* **17** (2001) 24.
[57] H.P. Tian, J.B. Yuan, Z.L. Zhu, L. Shi, C.H. Yang, M.E.A. Bekheet and C.L. Li // *J. Fuel Chem. Technol.* **25** (1997) 514.
[58] J. Yao, H. Wang, S.P. Ringer, K.Y. Chan, L. Zhang and N. Xu // *Micropor. Mesopor. Mater.* **85** (2005) 267.
[59] H.T. Wang, Z.B. Wang and Y.S. Yan // Chem. Commun. **23** (2000) 2333.
[60] H.T. Wang, L.M. Huang, Z.B. Wang, A. Mitra and Y.S. Yan // *Chem. Commun.* **15** (2001) 1364.
[61] H.T. Wang, B.A. Holmberg and Y.S. Yan // *J. Am. Chem. Soc.* **125** (2003) 9928.
[62] D. Chen, K. Moljord, T. Fuglerud and A. Holmen // *Micropor. Mesopor. Mater.* **29** (1999) 191.

[63] M.J. Van Niekerk, J.C.Q. Fletcher and C.T. O'Connor // *Appl. Catal. A* **138** (1996) 135.
[64] D. Chen, H.P. Rebo, A. Grønvold, K. Moljord and A. Holmen // *Micropor. Mesopor. Mater.* **121** (2000) 35.
[65] X. Wu and R.G. Anthony // *Appl. Catal. A* **218** (2001) 241.
[66] D. Chen, H.P. Rebo, K. Moljord and A. Holmen, In: C*atalyst Deactivation, Studies in Surface Science and Catalysis*, ed. by B. Delmon and J.T. Yates (Elsevier, Amsterdam, 1997), 159.
[67] Y.J. Lee, S.C. Baek and K.W. Jun // *Appl. Catal. A* **329** (2007) 130.
[68] A.M. Prakash and S. Unnikrishnan // *J. Chem. Soc. Faraday Trans.* **90** (1994) 2291.
[69] L. Marchese, A. Frache, E. Gianotti, G. Martra, M. Causa and S. Coluccia // *Micropor. Mesopor.Mater.* **30** (1999) 145.
[70] M. Mertens and K.G. Strohmaier, *US Patent 6696032 B2*, 2004.
[71] H. Van Heyden, S. Mintova and T. Bein // *Chem. Mater.* **20** (2008) 2956.
[72] V.K. La Mer and R.H. Dinegar // *J. Am. Chem. Soc.* **72** (1950) 4847.
[73] W. Xu, J. Dong, J. Li and F. Wu // *J. Chem. Soc. Chem. Commun.* **10** (1990) 755.
[74] M.H. Kim, H.X. Li and M.E. Davis // *Micropor. Mater.* **1** (1993) 191.
[75] M. Matsukata, N. Nishiyama and K. Ueyama // *Micropor. Mater.* **1** (1993) 219.
[76] P.R. Hari Prasad Rao, C.A. Leon, K. Ueyama and M. Matsukata // *Micropor. Mater.* **21** (1998) 305.
[77] S.K. Saha, S.B. Waghmode, H. Maekawa, R. Kawase, K. Komura, Y. Kubota and Y. Sugi // *Micropor. Mesopor. Mater.* **81** (2005) 277.
[78] B. Chen and Y. Huang // *Micropor. Mesopor. Mater.* **123** (2009) 71.
[79] Z. Yan, B. Chen and Y. Huang // *Solid State Magn. Reson.* **35** (2009) 49.
[80] Y. Hirota, K. Murata, S. Tanaka, N. Nishiyama, Y. Egashira and K. Ueyama // *Mater. Chem. Phys.* **123** (2010) 507.
[81] N. Nishiyama, M. Kawaguchi, Y. Hirota, D. Van Vu, Y. Egashira and K. Ueyama // *Appl. Catal. A* **362** (2009) 193.
[82] Y. Hirota, K. Murata, M. Miyamoto, Y. Egashira and N. Nishiyama // *Catal. Lett.* **1** (2010) 22.
[83] S. Lin, J. Li, R.P. Sharma, J. Yu and R. Xu // *Top. Catal.* **19** (2010) 1304.
[84] S.R. Venna and M.A. Carreon // *J. Phys. Chem. B* **51** (2008) 16261.
[85] M. Mertens and K.G. Strohmaier, *US Patent 6773688 B2*, 2004.
[86] L. Zhang, J. Yao, C. Zeng and N. Xu // *Chem. Comm.* **17** (2003) 2232.
[87] J. Yao, C. Zeng, L. Zhang and N. Xu // *Mater. Chem. Phys.* **112** (2008) 637.
[88] S.H. Jhung, J.S. Chang, J.S. Hwang and S.E. Park *//* *Micropor. Mesopor. Mater.* **1-3** (2003) 33.
[89] M. Gharibeh, G.A. Tompsett, W.C. Conner and K.S. Yngvesson // *Chem. Phys. Chem.* **9** (2008) 2580.
[90] K. Utchariyajit and S. Wongkasemjit // *Micropor. Mesopor. Mater.* **1-3** (2010) 116.
[91] S. Jianming, D.A. Jianwen and W. Laiping, *CN Patent 1356264A,* 2002.
[92] C. Liu, S.T. Wilson and B. McCulloch, *US Patent 0039554 A1,* 2008.